DELAYED MODE QUALITY CONTROL OF ARGO SALINITY DATA IN THE MEDITERRANEAN AND BLACK SEA

FLOAT WMO 6900818

G. Notarstefano and P.-M. Poulain

Produced by the Mediterranean Argo Regional Centre (MedArgo), OGS, Trieste, Italy

February 3rd, 2012

1. Float data

The float data were downloaded on January 2012 from the Coriolis Data centre IFREMER (a GDAC centre), Brest, France, in NetDCF format. The data were converted in Matlab binary file.

2. Status of the float

The float was deployed far West of Crete in the Ionian Sea (Figure 1), in October 2009 and performed just less than 60 cycles (Table 1). The salinity and temperature sections along the float trajectory are depicted in Figures 2 and 3, respectively.

Model	WMO	Argos	Deploy Date	Lat	Lon	Cycle	Last Date	Lat	Lon	Status
Nemo 084	6900818	82687	16-Oct-2009 19:22	36.17	21	57	28-Jul-2010 15:49	30.89	29.12	Dead

Table 1. Status of the float.

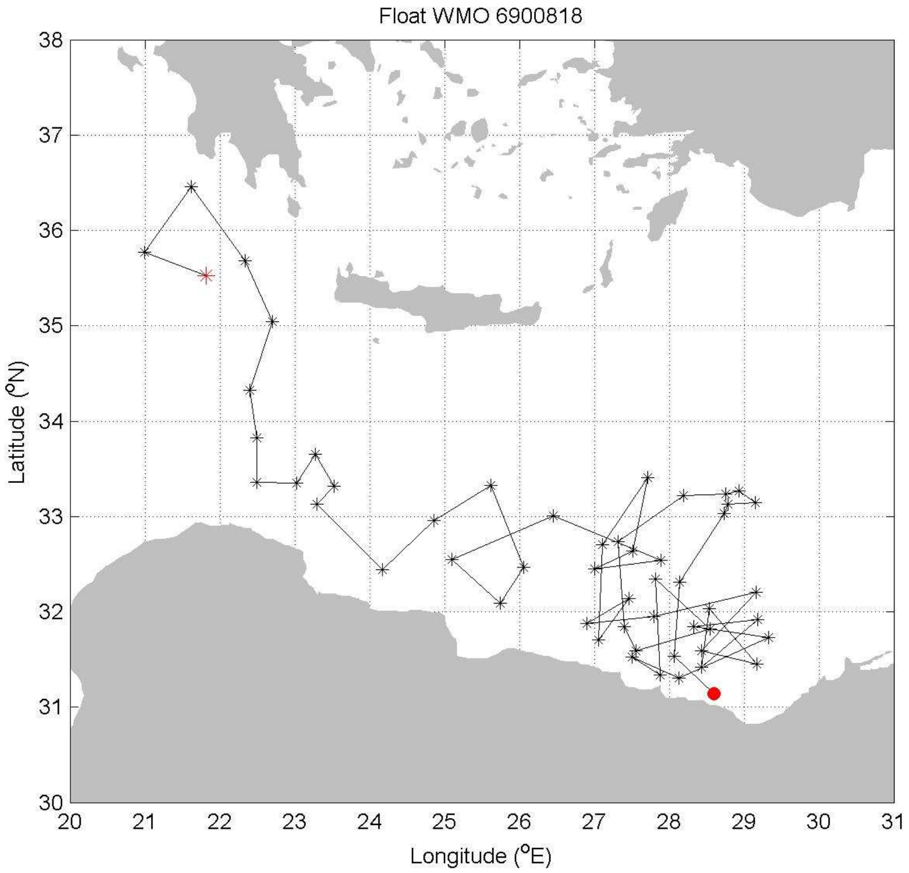

Figure 1. Float trajectory (the red dot represents the last float position).

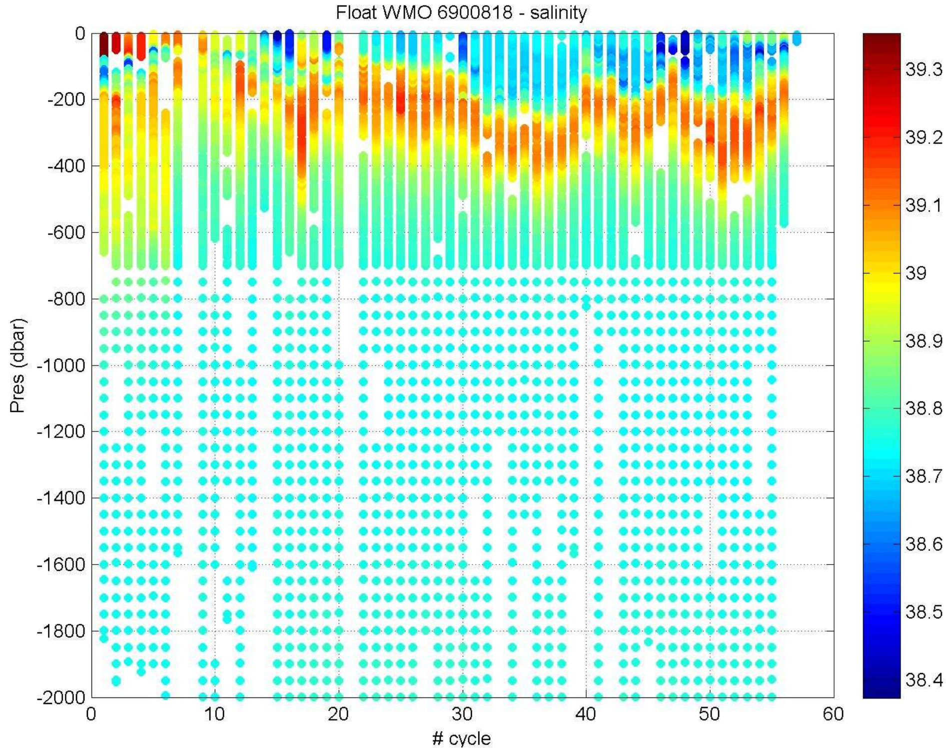

Figure 2. Salinity section along the float trajectory.

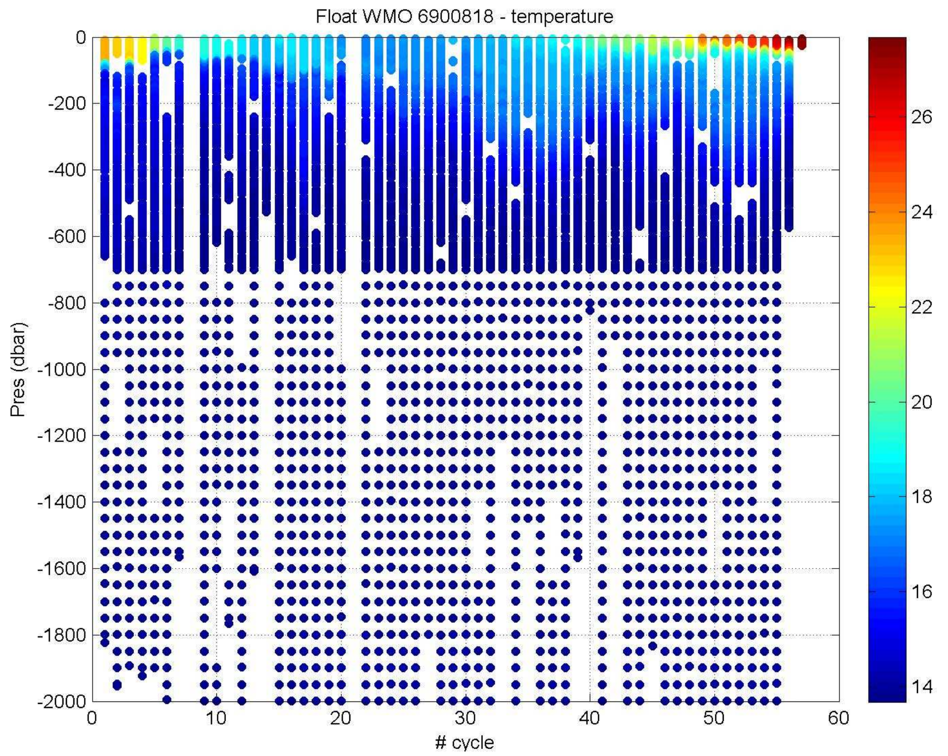

Figure 3. Temperature (° C) section along the float trajectory.

3. Surface pressure

The adjusted surface pressure is plotted in Figure 4. Surface pressure is extracted from the Argo technical file: the variable name is "IfremerTemporaryCode_PRES_SurfacePressure_dBAR". No adjustment of the CTD pressure profiles is required because the correction is much less than the manufacturer quoted accuracy of the pressure sensor (2.4 dbar).

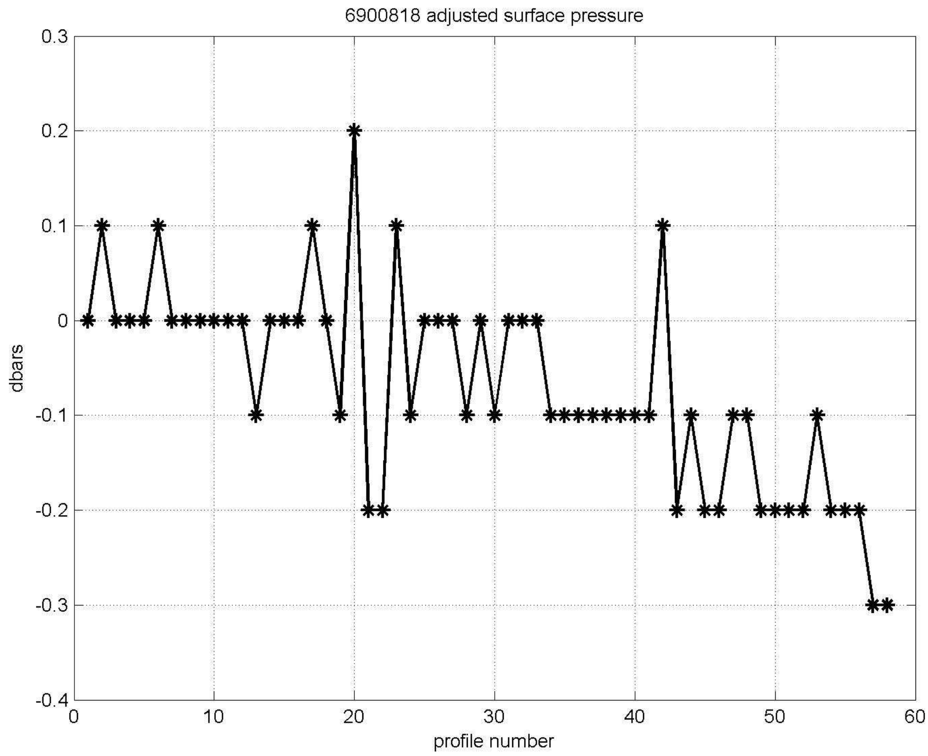

Figure 4. Adjusted surface pressure values versus time.

4. Manual inspection and identification of major spikes in temperature and salinity

No major spikes or jumps were detected in both temperature (Figure 5) and salinity (Figure 6) profiles.

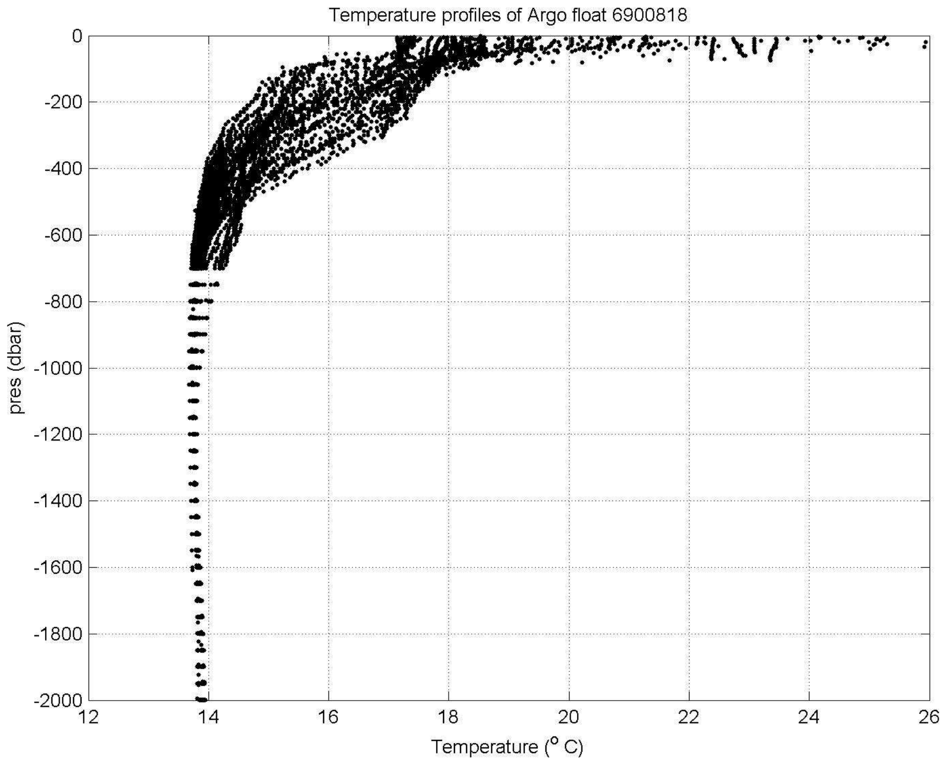

Figure 5. Temperature profiles as they are in real time correction mode at Coriolis Data Centre.

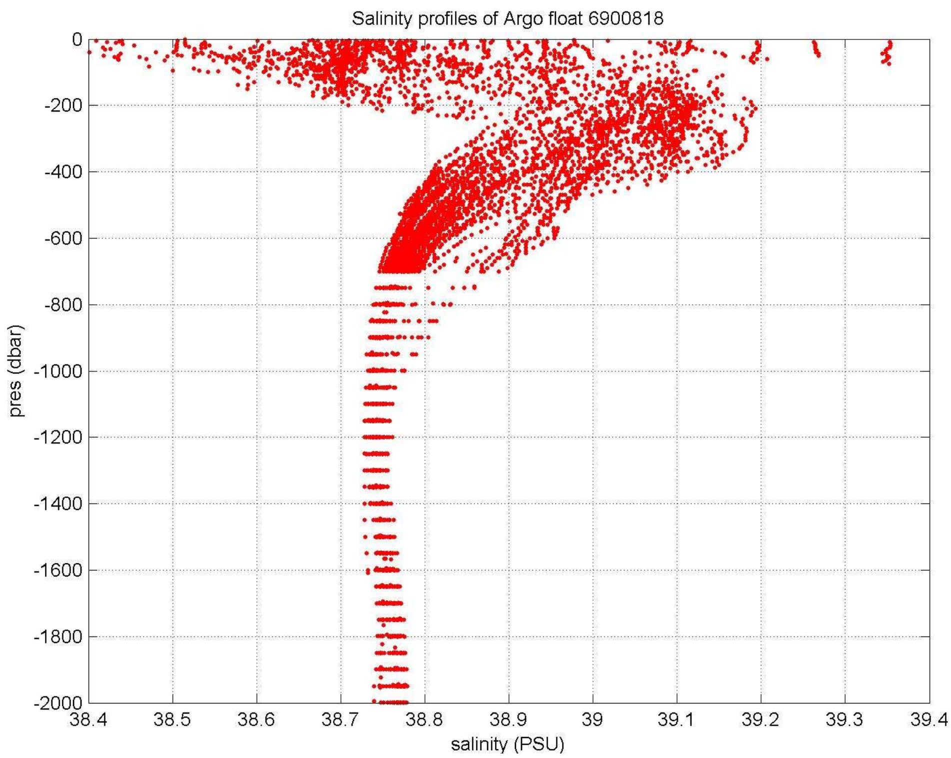

Figure 6. Salinity profiles as they are in real time correction mode at Coriolis Data Centre.

5. Reference dataset

The reference data used in the delayed mode quality control (DMQC) method, as of January 2012, are composed of the following CTD and Argo historical datasets (see the historical locations in Figure 7):

- Ref. Database Eflubio-2 (2005)
- Ref. Database Eflubio-3 (2004)
- Ref. Database CTD_for_DMQC_2010V2 (1970-2008)
- Ref. Database Egitto-1 (2006)
- Ref. Database Enea (Borghini – 2004-2006)
- Ref. Database Enea (Santoleri - 2004)
- Ref. Database MFSTEP (2003)
- Ref. Database MREA07 – IT_NAVY Aretusa (2007)
- Ref. Database MREA07 – IT_NAVY Galatea (2007)
- Ref. Database MREA07 – NURC Leonardo (2007)
- Ref. Database MREA07 NURC Leonardo LASIE07 (2007)
- Ref. Database MREA07 – TNO Snellius (2007)
- Ref. Database NODC odv-1 (2000)
- Ref. Database NODC odv-2 (2006)
- Ref. Database SESAME IT2 (2008)
- Ref. Database IT6 SESAME (2008)
- Ref. Database MEADAR/MEDATLAS (1975-1997)
- Ref. Database SINAPSI (1997-2002)
- Ref. Database METEOR/URANIA 1999 (1999)
- Ref. Database TRANSMED (2007)
- Ref. Database ARGO_for_DMQC_2011V4 (2002-2011)

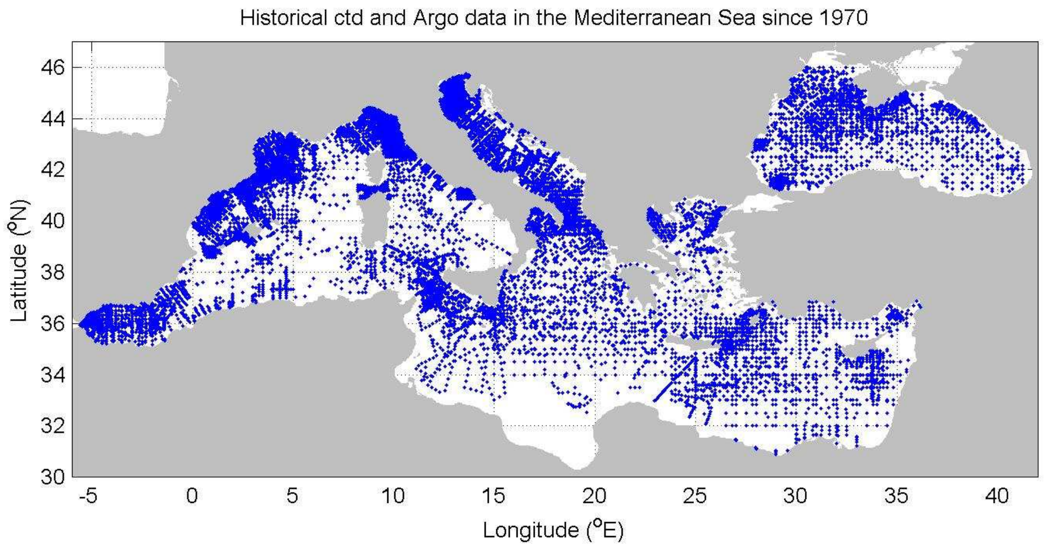

Figure 7. Location of the historical CTD and Argo data, spanning from 1970 to 2011, used in the DMQC.

6. Qualitative comparison between float and historical CTD profiles

In Figure 8 the float trajectory and the historical CTD locations are plotted. The salinity profiles of the Argo float are superimposed on the spatially closest historical profiles in Figure 9.

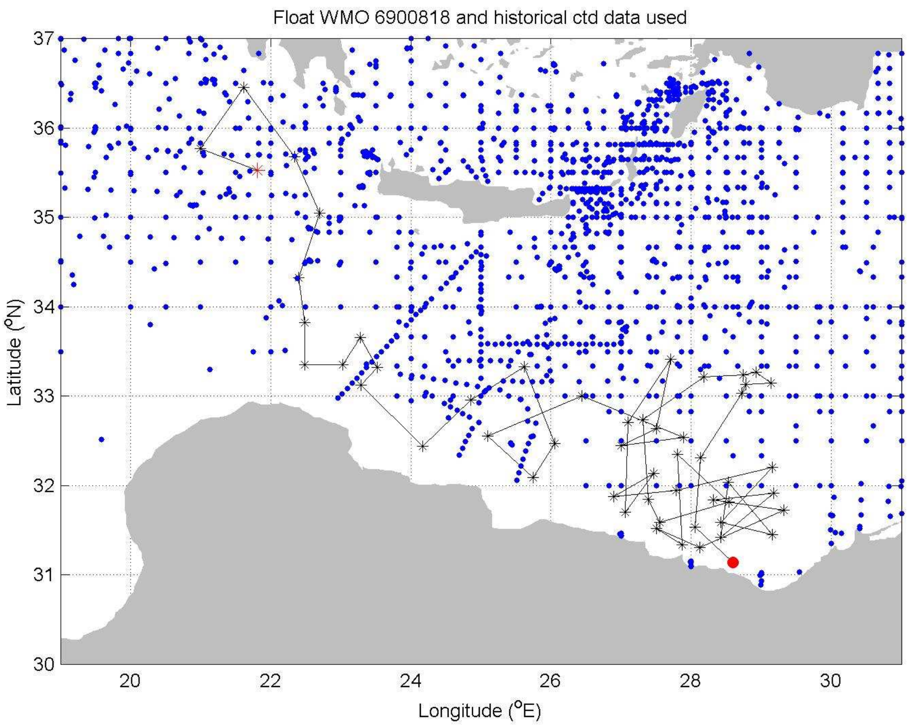

Figure 8. Float trajectory (black line; the last float position is depicted by a red dot) and locations of the historical CTD data.

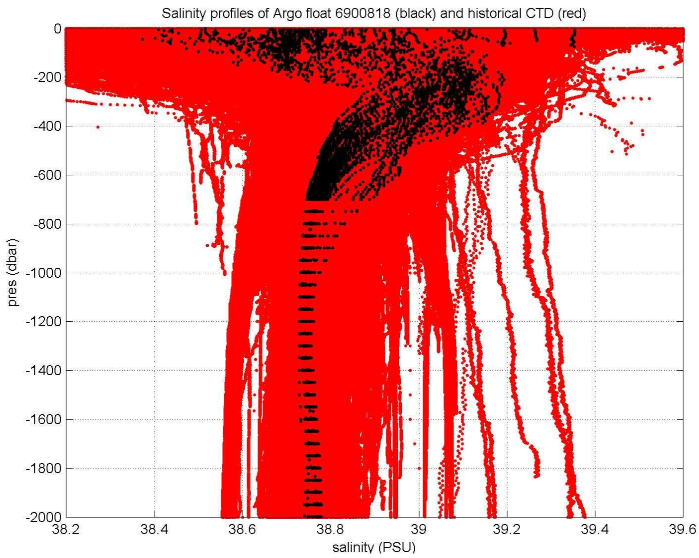

Figure 9. Salinity profiles of the Argo float (black lines) and historical CTD (red lines).

In Figure 10, three float profiles are selected to perform a comparison (in time and space) with the historical data. The float profile is depicted in black while other colours represent the reference profiles. The red colour means that the historical data are more recent with respect to the float ones, while magenta states that the float data are more recent than the historical ones (the maximal difference is 3 years). A time difference between 3 and 6, 6 and 9 and larger than 9 years is depicted in green, cyan and blue, respectively.

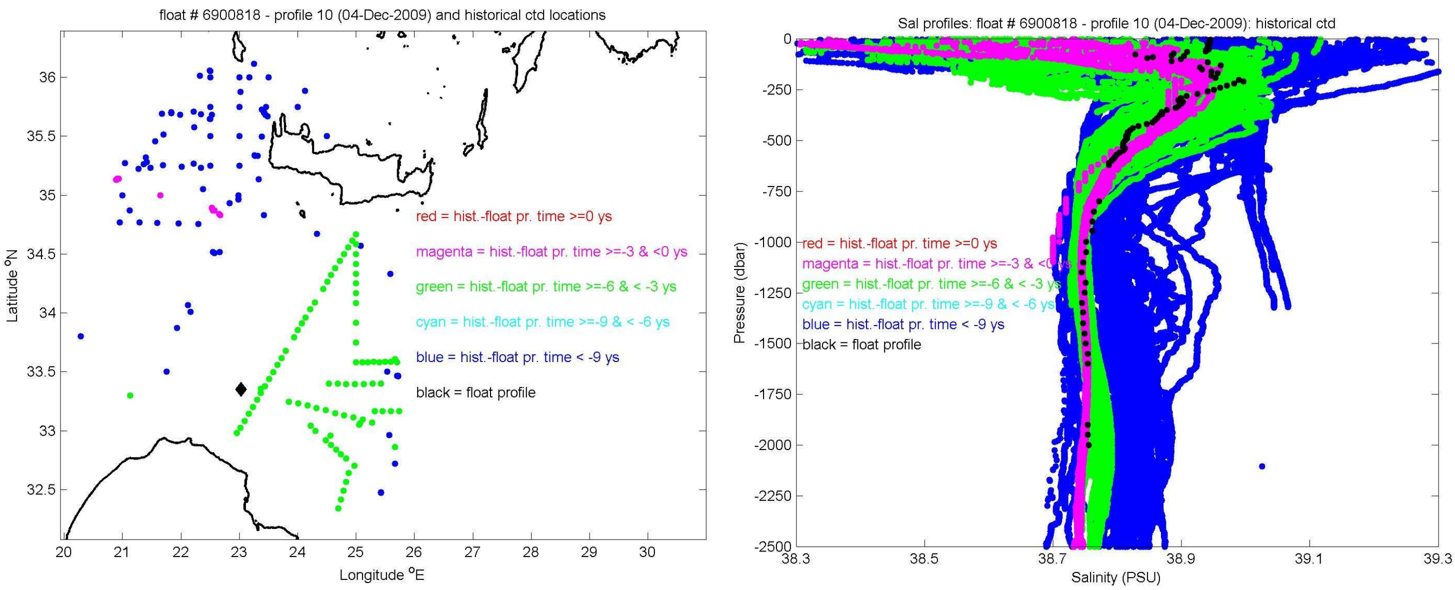

Figure 10. Location of selected float profiles and historical CTD data (left panels) and the respective salinity profiles (right panels).

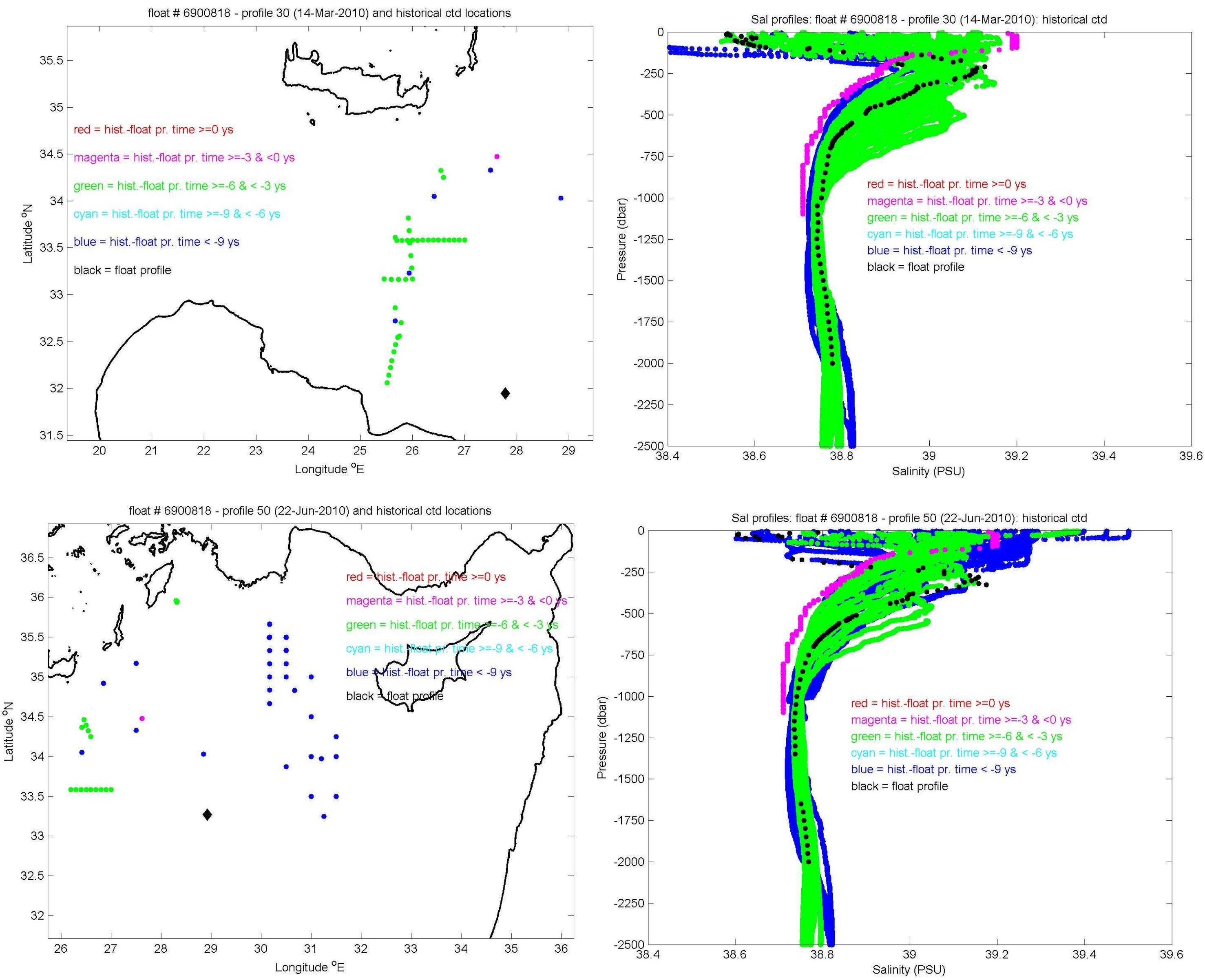

Figure 10. Continued.

The smallest temporal difference between the two datasets is observed for the float profile number 10: the float data are more recent than the historical ones by about 692 days.

7. DMQC: configuration and results

We applied the DMQC method of Owens and Wong, referred to as OW hereafter (Owens and Wong, 2009) to floats operating in the Mediterranean and Black Sea (Notarstefano and Poulain, 2008). The parameters used for the objective mapping are listed in Table 2. A maximum of 4 break points are allowed in the piece-wise linear fit.

Parameters	Value
CONFIG_MAX_CASTS	300
MAP_USE_PV	1
MAP_USE_SAF	0
MAPSCALE_LONGITUDE_LARGE	6
MAPSCALE_LONGITUDE_SMALL	2
MAPSCALE_LATITUDE_LARGE	5
MAPSCALE_LATITUDE_SMALL	1.67
MAPSCALE_PHI_LARGE	0.5
MAPSCALE_PHI_SMALL	0.1
MAPSCALE_AGE	1
MAP_P_EXCLUDE	200
MAP_P_DELTA	250

Table 2. Objective mapping parameters of the OW method.

The results of the OW method are presented in Figures from 11 to 14. The 10 θ-levels chosen for the correction are reported in Figure 11. The corrected and uncorrected float salinity and the mapped salinity on θ-levels are depicted in Figure 12. The float data corrected by the OW method are presented in Figure 13. The correction proposed (Figure 14) is between -0.01 and 0.01 PSU; the correction term ***r*** is computed by the piece-wise liner fit and the additive correction ***ΔS*** is calculated using:

$$\Delta S = (r-1)\cdot C_0 + (r-1)\cdot C'$$

where C_0 is the vertical mean conductivity and C' is the variation around C_0.

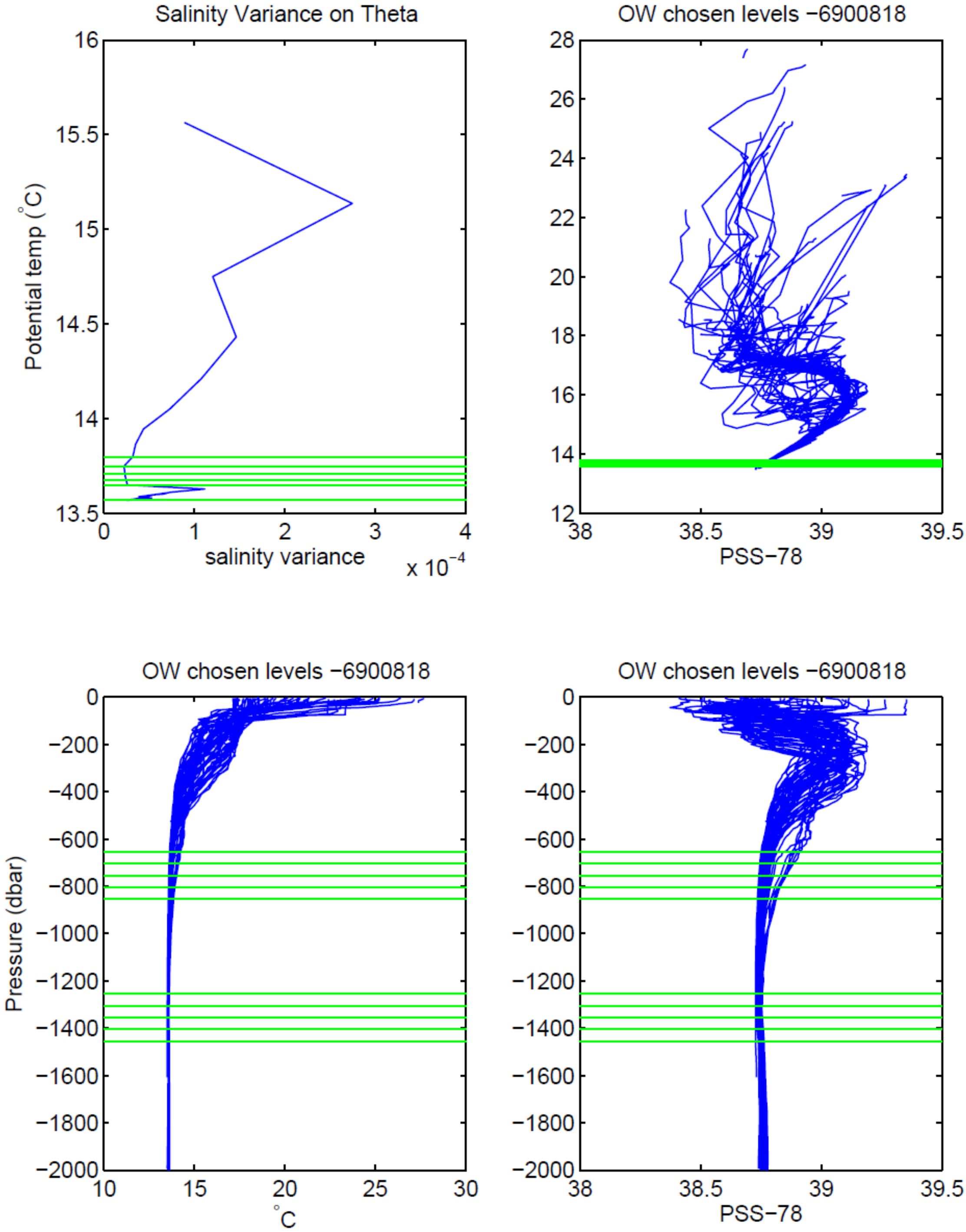

Figure 11. The 10 θ-levels chosen for the correction.

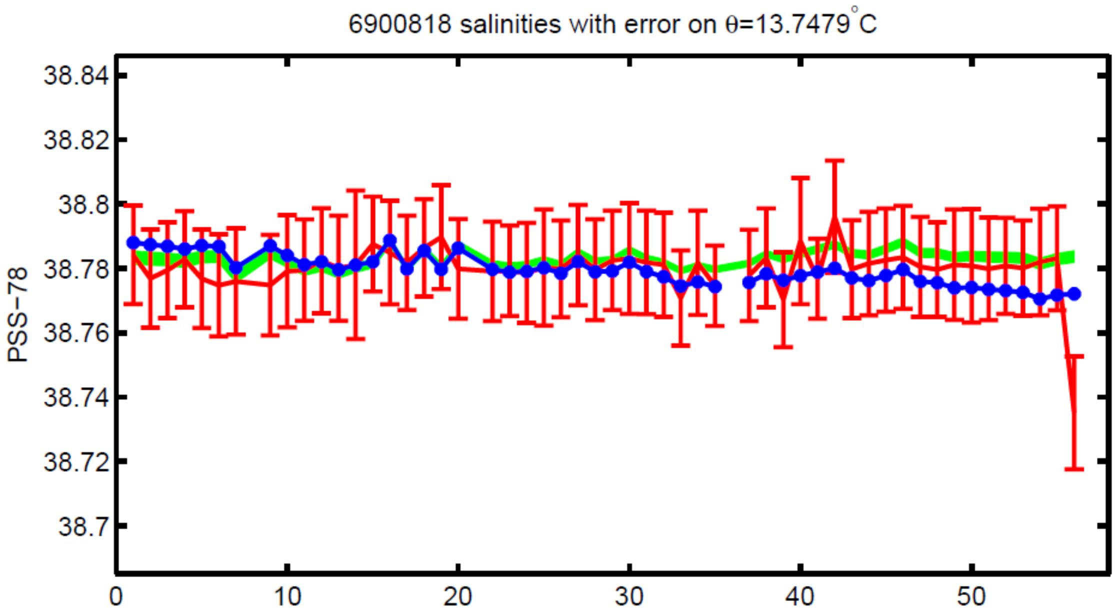

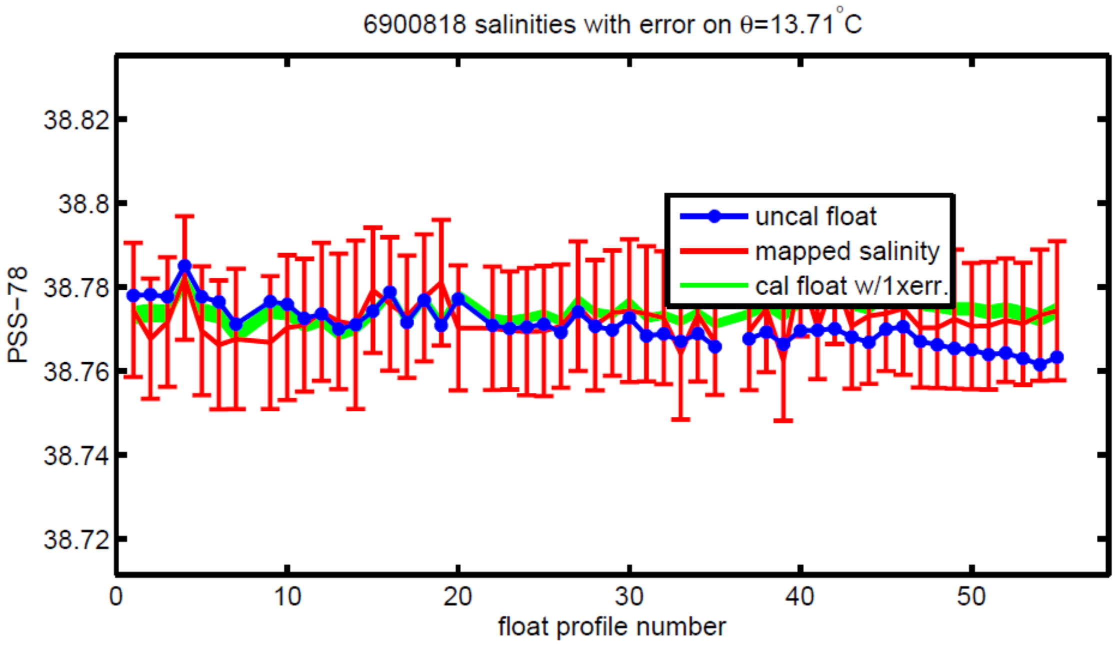

Figure 12. Comparison between the float salinity data and the mapped salinity, on θ-levels.

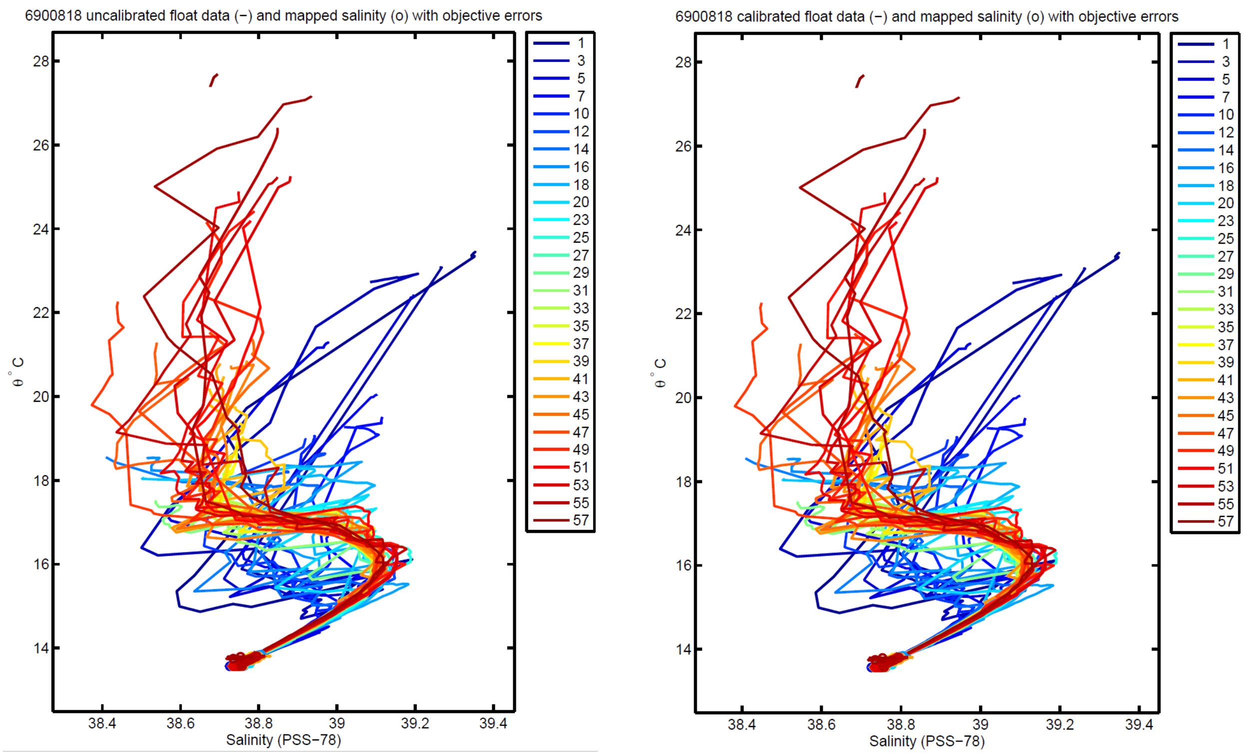

Figure 13. θ-S diagram of uncorrected (left) and corrected data (right).

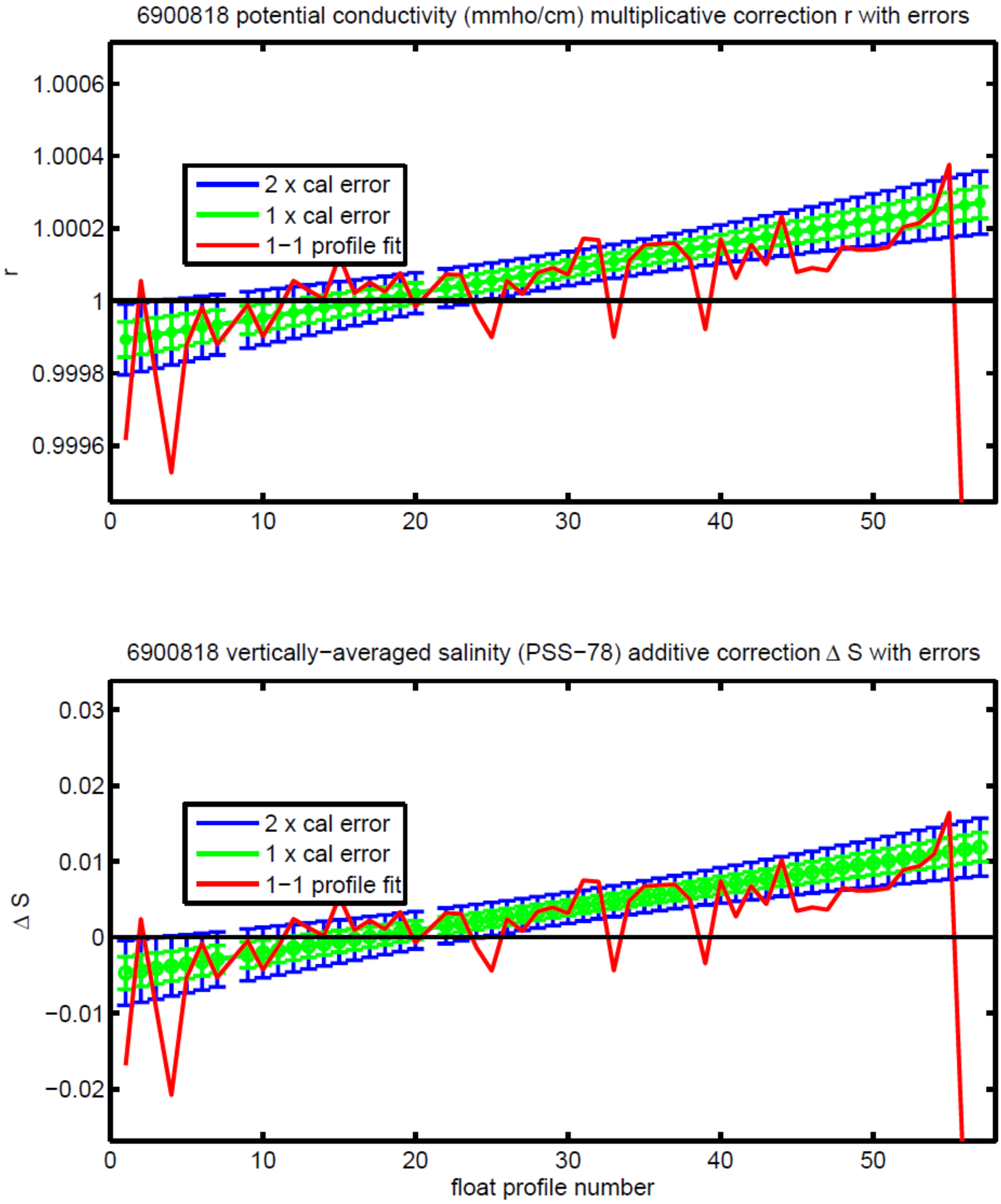

Figure 14. Correction proposed by the OW method.

The observations in the θ-S diagram of profile segments deeper than 700 dbar (Figure 15) show that the tightest θ-S relationship is just below this depth. Hence, the analysis of this portion of the θ-S curve can be useful to detect the sensor accuracy.

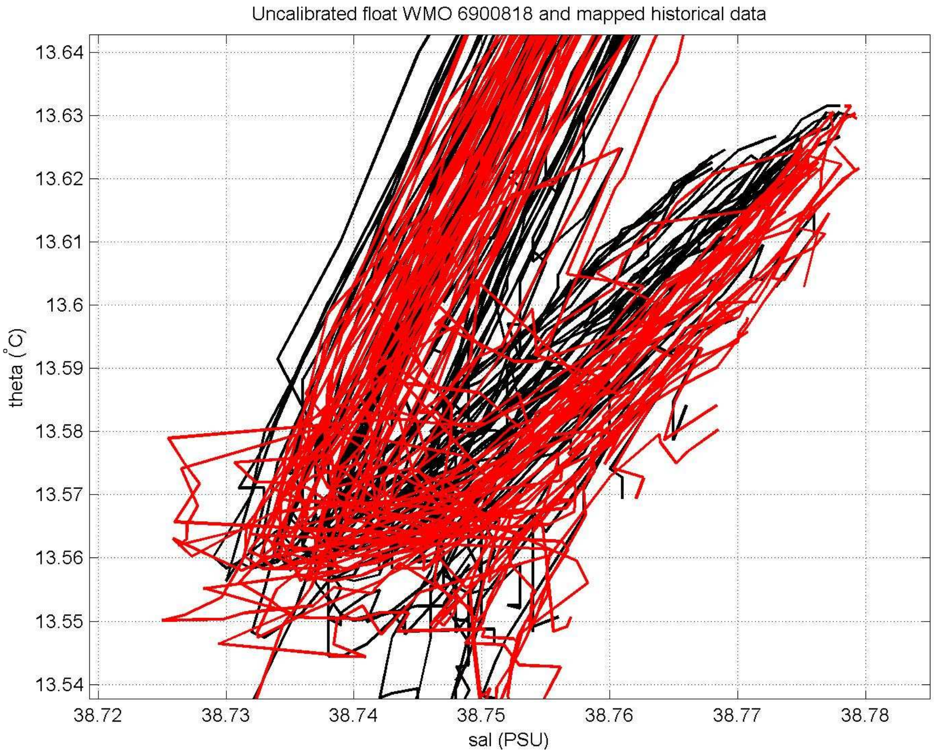

Figure 15. Uncalibrated float salinity profiles (black lines) and mapped historical data (red lines) in the most uniform part of the θ-S curve.

8. Conclusions

The correction proposed (Figure 14) is between -0.01 and 0.01 PSU and hence comparable to the Argo accuracy (±0.01 PSU). The float salinity profiles are also enclosed by the historical profiles and this means that any potential salinity drift is smaller than the variability of the reference dataset. In the most uniform section of the θ-S curve (Figure 15) the variability of the float salinity is around 0.01 PSU and this is an indication that salinity measurements from this Argo float are accurate to within 0.01 PSU (potential drift). A more precise analysis reveals that the mapped historical salinities are almost comparable to the float data (Figure 15): this confirms that there is no need to calibrate the sensor. Moreover, the deep selected float salinity profiles (Figure 10) are in a good agreement with the closest (in time) historical profiles. We can conclude that there is no evidence of a potential salinity drift in the float measurements. Hence, the salinity data of Float WMO 6900818 can be considered of good quality and no delayed mode correction is deemed necessary.

References

Notarstefano G. and Poulain P.-M. (2008). Delayed mode quality control of Argo floats salinity data in the Tyrrhenian Sea. Rel 2008/125 OGA 43 SIRE, Trieste, Italy, 33 pp.

Owens W. B. and Wong A. P. S. (2009). An improved calibration method for the drift of the conductivity sensor on autonomous CTD profiling floats by θ-S climatology, Deep Sea Research Part I: Oceanographic Research Papers, 56(3), 450-457.